

This article was downloaded by:

On: 29 January 2011

Access details: *Access Details: Free Access*

Publisher *Taylor & Francis*

Informa Ltd Registered in England and Wales Registered Number: 1072954 Registered office: Mortimer House, 37-41 Mortimer Street, London W1T 3JH, UK



## Supramolecular Chemistry

Publication details, including instructions for authors and subscription information:

<http://www.informaworld.com/smpp/title~content=t713649759>

### Conformational Studies of Dibenzo-30-crown-10 Complexes. Syntheses and Crystal Structures of Potassium and Ammonium Hexafluorophosphate Complexes

Ivanka Matijašić<sup>a</sup>; Paolo Dapporto<sup>b</sup>; Patrizia Rossi<sup>b</sup>; Ljerka Tušek-Božić<sup>c</sup>

<sup>a</sup> Laboratory of Organic Chemistry, Faculty of Science, University of Zagreb, Zagreb, Croatia <sup>b</sup>

Department of Energetics "Sergio Stecco", University of Florence, Florence, Italy <sup>c</sup> Department of Physical Chemistry, Ruder Bošković Institute, Zagreb, Croatia

**To cite this Article** Matijašić, Ivanka , Dapporto, Paolo , Rossi, Patrizia and Tušek-Božić, Ljerka(2001) 'Conformational Studies of Dibenzo-30-crown-10 Complexes. Syntheses and Crystal Structures of Potassium and Ammonium Hexafluorophosphate Complexes', *Supramolecular Chemistry*, 13: 1, 193 – 206

**To link to this Article:** DOI: 10.1080/10610270108034894

**URL:** <http://dx.doi.org/10.1080/10610270108034894>

PLEASE SCROLL DOWN FOR ARTICLE

Full terms and conditions of use: <http://www.informaworld.com/terms-and-conditions-of-access.pdf>

This article may be used for research, teaching and private study purposes. Any substantial or systematic reproduction, re-distribution, re-selling, loan or sub-licensing, systematic supply or distribution in any form to anyone is expressly forbidden.

The publisher does not give any warranty express or implied or make any representation that the contents will be complete or accurate or up to date. The accuracy of any instructions, formulae and drug doses should be independently verified with primary sources. The publisher shall not be liable for any loss, actions, claims, proceedings, demand or costs or damages whatsoever or howsoever caused arising directly or indirectly in connection with or arising out of the use of this material.

# Conformational Studies of Dibenzo-30-crown-10 Complexes. Syntheses and Crystal Structures of Potassium and Ammonium Hexafluorophosphate Complexes\*

IVANKA MATIJAŠIĆ<sup>a,†</sup>, PAOLO DAPPORTO<sup>b</sup>, PATRIZIA ROSSI<sup>b</sup> and LJERKA TUŠEK-BOŽIĆ<sup>c</sup>

<sup>a</sup>Laboratory of Organic Chemistry, Faculty of Science, University of Zagreb, 10000 Zagreb, Strossmayerov trg 14, Croatia;

<sup>b</sup>Department of Energetics "Sergio Stecco", University of Florence, via S. Marta 3, 50139 Florence, Italy; <sup>c</sup>Department of Physical Chemistry, Ruder Bošković Institute, Bijenička 54, 10002 Zagreb, Croatia

Crown ether complexes formed by the dibenzo-30-crown-10 (DB30C10) with potassium and ammonium hexafluorophosphate have been prepared and their crystal structures have been determined by single crystal X-ray analyses. The potassium complex (compound 1) consists of  $[K(DB30C10)]^+$  cation and  $PF_6^-$  anion. Crystals are monoclinic, space group  $P2_1/n$ , with  $a = 11.9106(3)$ ,  $b = 9.8382(5)$ ,  $c = 14.3062(3)$  Å,  $\beta = 97.581(3)^\circ$ ,  $V = 1661.7(1)$  Å<sup>3</sup>,  $D_c = 1.440$  g cm<sup>-3</sup>,  $Z = 4$ ,  $R = 0.0675$  for 2528 unique observed reflections. The potassium atom is coordinated to the ten oxygen atoms of the crown ligand at the distance from 2.859(3) to 2.930(3) Å. The ammonium complex (compound 2) has also 1:1 crown-cation ratio. Crystals are monoclinic, space group  $P2_1/n$ , with  $a = 12.5061(6)$ ,  $b = 19.3724(5)$ ,  $c = 14.2203(9)$  Å,  $\beta = 102.476(5)^\circ$ ,  $V = 3363.8(3)$  Å<sup>3</sup>,  $D_c = 1.501$  g cm<sup>-3</sup>,  $Z = 4$ ,  $R = 0.0677$  for 4172 unique observed reflections. The ammonium cation is completely enclosed with crown oxygen atoms forming seven hydrogen bonds. The conformation of previously reported dibenzo-30-crown-10 complexes with potassium salts were investigated using polar coordinate maps.

**Keywords:** Dibenzo-30-crown-10 complexes; Crystal structure; Conformation; Molecular recognition; Hydrogen bonding

## INTRODUCTION

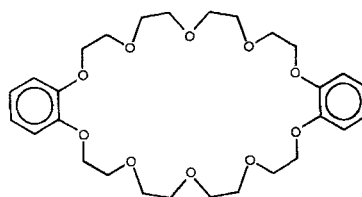
One of the most important areas of supramolecular chemistry that has developed over the past two decades is the metal-ion and host-guest chemistry of macrocyclic ligands, which have utility in different fields and now also considerable biochemical relevance as model substances of naturally occurring ionophores for the study of ion-transport processes in cell membranes [1]. The chemistry of metal-ion macrocyclic complexes and the structures they adopt, in the solid state and in solution, are influenced by a variety of factors, including the size and ionic character of the metal ion and the flexibility and cavity size of the macrocycle. All these factors must be taken into account when tailoring ligands to recognize particular metal ions. Much research effort has centered on understanding the effect of altering the nature of the metal or ligand on the stoichiometry and structure of the complexes formed [2].

\*Dedicated to Professor Fumio Toda on the occasion of his 67th birthday.

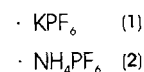
<sup>†</sup>Corresponding author. e-mail: matijas@rudjer.irb.hr

The smaller crown ethers with a planar polyether cavity (such as 18-crown-6), although they bind potassium selectively, have been found to be less effective ionophores for potassium than the natural systems, since two sides of the crown complex are not as well protected from the hydrophobic environment existing in the membrane. A better synthetic model is larger crown ethers, such as dibenzo-30-crown-10 (DB30C10), since this highly flexible ligand could completely enclose the metal cation similarly to the naturally occurring cyclic ionophores. The combination of a conformational mobility allied with the large cavity size of dibenzo-30-crown-10 provides a complexation profile of high coordination metal geometry [3]. It was noted that this oxacrown ligand can easily wrap itself around a metal ion such as the s-block cations  $M^+$  ( $M = K, Rb$ ) [4–7] and  $M^{2+}$  ( $M = Ba$ ) [8,9], so that the polyether ring completely encircles the central metal ion with all ten oxygen atoms involved in bonding interactions. Evidence of such structures was also found in solution for the  $Ag^+$  and  $Tl^+$  ions [10]. This crown ether can also accommodate two smaller cations if the repulsion forces are not so large, as in the case of the sodium thiocyanate complex in which two  $Na^+$  cations are symmetrically entrapped within the polyether cavity [11]. Some transition metal liquid clathrates contain the oxonium ion-crown ether complexes with two  $H_3O^+$  ions coordinated to the 30-membered macrocycle [12].

In this paper we describe complexation of dibenzo-30-crown-10 with potassium and ammonium hexafluorophosphate, as a part of our systematic investigation of the alkali and ammonium hexafluorophosphate salt complexes with different crown ethers both in solution [13] and in the solid state [14, 15].



SCHEME 1



## EXPERIMENTAL

### Materials

Dibenzo-30-crown-10<sup>1</sup> was used directly as supplied (Aldrich). Ammonium and potassium hexafluorophosphates (Aldrich) were purified by recrystallization from absolute ethanol and water, respectively, and dried under vacuum at 25°C for 10 h [16,17]. Analytical grade methanol was used for preparation of the salt complexes.

### Preparation of the Complexes

An equimolar amount of crown ether dibenzo-30-crown-10 (DB30C10) and hexafluorophosphate salt ( $KPF_6$ ,  $NH_4PF_6$ ; respectively) was dissolved in methanol and refluxed for 3–5 h with vigorous stirring. The clear hot solution was filtered hot and allowed to stand at room temperature. The crystalline precipitate gradually formed was filtered off, washed with cold methanol and dried under vacuum overnight. The filtered solution was subjected to slow solvent evaporation in a desiccator over  $P_2O_5$ . Complexes isolated as white crystals were characterized by microanalytical and spectroscopic (IR and  $^1H$  NMR) data.

$K(DB30C10)PF_6$  (1). Yield 82%, M.p. 188–189°C. Anal. Found: C, 46.8; H, 5.4; P, 4.5%. Calc.

<sup>1</sup>IUPAC name is 6,7,9,10,12,13,15,16,23,24,26,27,29,30,32,33-hexadecahydrodibenzo[*b,q*][1,4,7,10,13,16,19,22,25,28]decaoxacyclotriacontine.

for  $C_{28}H_{40}KO_{10}PF_6$ : C, 46.6; H, 5.6; P, 4.3%. Selected IR data (KBr,  $cm^{-1}$ ): 1258 s, 1211 m ( $\nu_{as}Ar-O-CH_2$ ); 1118 s, 1100 m ( $\nu_{CH_2-O-CH_2}$ ); 1083 m, 1050 m ( $\nu_s Ar-O-CH_2$ ); 934 m, 921 m ( $\omega, \tau CH_2$ ); 839 vs, 558 m-s ( $\nu PF_6$ ).  $^1H$  NMR (DMSO- $d_6$ ):  $\delta$  3.57 (m, 8 H, 4- $CH_2$ ), 3.61 (m, 8 H, 3- $CH_2$ ), 3.73 (s br, 8 H, 2- $CH_2$ ), 4.07 (s br, 8 H, 1- $CH_2$ ), 6.90 (m, 4 H,  $\beta$ -ArH), 6.95 (m, 4 H,  $\alpha$ -ArH).

$NH_4(DB30C10)PF_6$  (2). Yield 80%, M.p. 159–160°C. Anal. Found: C, 48.2; H, 6.5; N, 2.1; P, 4.2%. Calc. for  $C_{28}H_{44}NO_{10}PF_6$ : C, 48.1; H, 6.3; N, 2.0; P, 4.4%. Selected IR data (KBr,  $cm^{-1}$ ): 3256 vs ( $\nu NH_4^+$ ); 1257 s, 1210 m-s ( $\nu_{as} Ar-O-CH_2$ ); 1118 s, 1093 s ( $\nu_{CH_2-O-CH_2}$ ); 1048 s ( $\nu_s Ar-O-CH_2$ ); 936 m, 920 sh ( $\omega, \tau CH_2$ ); 839 vs br, 558 s ( $\nu PF_6$ ).  $^1H$  NMR (DMSO- $d_6$ ):  $\delta$  3.56 (m, 8 H, 4- $CH_2$ ), 3.62 (m, 8 H, 3- $CH_2$ ), 3.74 (t, 8 H,

2- $CH_2$ ), 4.06 (t, 8 H, 1- $CH_2$ ), 6.89 (m, 4 H,  $\beta$ -ArH), 6.94 (m, 4 H,  $\alpha$ -ArH), 7.10 (s, 4 H,  $NH_4^+$ ).

### Physical Measurements and Analyses

Melting points were determined on a hot-stage microscope and are uncorrected. Infrared spectra were obtained on a Perkin-Elmer 580B spectrophotometer using KBr pellets.  $^1H$  NMR spectra were recorded on a Varian 300 Gemini spectrometer. Samples were dissolved in DMSO- $d_6$  at 298 K in 5 mm tubes, containing tetramethylsilane as an internal reference. Digital resolution was 0.25 Hz. The NOESY spectra were obtained in a phase-sensitive mode with 1 K by 1 K size and 128 increments. Each increment was obtained with 16 scans, using 5000 Hz spectral width, relaxation delay of 1 s

TABLE I Crystal data and structure refinement details

Compound	1	2
Empirical formula	$C_{14} H_{20} F_3 K_{0.5} O_5 P_{0.5}$	$C_{14} H_{20} F_3 K_{0.5} O_5 P_{0.5}$
Molecular weight	360.33	699.61
Space group	$P 2_1/n$	$P 2_1/n$
<i>a</i> (Å)	11.9106(3)	12.5061(6)
<i>b</i> (Å)	9.8382(5)	19.3724(5)
<i>c</i> (Å)	14.3062(3)	14.2203(5)
$\beta$ (°)	97.581(3)	102.476(5)
<i>V</i> (Å <sup>3</sup> )	1661.7(1)	3663.8(3)
<i>Z</i>	2	4
<i>D<sub>c</sub></i> (Mg m <sup>-3</sup> )	1.440	1.472
Radiation	CuK $\alpha$	CuK $\alpha$
<i>F</i> (000)	752	1472
$\mu$ (mm <sup>-1</sup> )	2.630	1.501
<i>T</i> (K)	293(2)	293(2)
Crystal size (mm)	0.57 × 0.32 × 0.20	0.60 × 0.41 × 0.25
$\theta$ range (°)	4.49 – 64.19	3.92 – 59.82
Index ranges	–12 < <i>h</i> < 13 0 < <i>k</i> < 11 0 < <i>l</i> < 16	–14 < <i>h</i> < 1 –1 < <i>k</i> < 20 –14 < <i>l</i> < 15
Scan mode	$\theta - 2\theta$	$\theta - 2\theta$
Reflections collected	3299	5239
Reflections observed	2528 [ <i>I</i> > 2 $\sigma$ ( <i>I</i> )]	4175 [ <i>I</i> > 2 $\sigma$ ( <i>I</i> )]
Refined parameters	213	417
Goodness of fit on <i>F</i> <sup>2</sup>	0.994	1.023
<i>R</i> <sub>1</sub> / <i>wR</i> <sub>2</sub> indices (obs. data)	0.0675 / 0.2059	0.0700 / 0.1874
<i>R</i> <sub>1</sub> / <i>wR</i> <sub>2</sub> indices (all data)	0.0745 / 0.2191	0.0961 / 0.2123
Extinction coefficient	0.0002(4)	0.0003(1)
$\Delta\rho_{max, min}$ (e Å <sup>-3</sup> )	0.424, –0.320	0.562, –0.250
( $\Delta/\rho$ ) <sub>max</sub>	0.002	0.001

and mixing time of 0.45 s. Elemental analyses were performed in the Microanalytical Laboratory of the Ruder Bošković Institute.

### Structure Determination and Refinement

Suitable crystals of both complexes were obtained by recrystallization from dry methanol solution. The cell parameters and intensity data were measured on a Siemens P4 diffractometer with graphite monochromated Cu K $\alpha$  radiation ( $\lambda = 1.54178 \text{ \AA}$ ). The accurate cell parameters were obtained by least-squares analyses of 25 reflections measured in the range  $10^\circ < \theta < 18^\circ$ . Crystal data and experimental details of the data collections are listed in Table I.

The structures were determined by direct methods and refined by full-matrix least-squares routines using the SIR92 and SHELX97 programs [18, 19]. The non-hydrogen atoms were treated anisotropically, while hydrogen atoms were introduced in calculated positions and refined riding on their respective carbon atoms with a common isotropic thermal displacement parameter. The ammonium hydrogens in compound **2** were located by difference electron density map and refined with a simple bond length constraint to the nitrogen atom.

There is evidence in the large thermal factors for some of the carbon atoms in the ligand, especially of complex **2**, but separate sites could not be found on  $\Delta F$  maps. Probably for this reason the C21–C22 distance converged to 1.233(11)  $\text{\AA}$ . We conclude the refinement with a constraint bond length at the value of 1.386(8)  $\text{\AA}$  and other details as given in Table I. An empirical absorption was applied using DIFABS [20]. Drawings were prepared by the ORTEP-3 and PLUTON-98 programs [21, 22]. The fractional atomic coordinates and equivalent thermal factors of compound **1** and **2** are listed in Tables II and III. Selected bond distances and torsion angles are given in Tables IV and V. Hydrogen bonding geometry for **2** is listed in Table VI. Supplementary material comprises hydrogen coordinates, anisotropic thermal

TABLE II Atomic coordinates and equivalent isotropic displacement parameters for **1**

Atom	<i>x</i>	<i>y</i>	<i>z</i>	<i>U</i> (eq)
K1	0.7500	0.1268(1)	0.2500	0.056(1)
P1	0.7500	0.3988(1)	−0.2500	0.064(1)
F1	0.7500	0.2388(4)	−0.2500	0.118(2)
F2	0.7500	0.5570(4)	−0.2500	0.130(2)
F3	0.6393(3)	0.3974(3)	−0.3244(2)	0.101(1)
F4	0.8241(3)	0.3969(4)	−0.3342(2)	0.125(1)
O1	0.8448(2)	0.1028(2)	0.0719(2)	0.063(1)
O2	0.7665(3)	0.3595(3)	0.1308(2)	0.079(1)
O3	0.5522(3)	0.2737(5)	0.1725(2)	0.100(1)
O4	0.5642(3)	−0.0106(4)	0.1403(2)	0.097(1)
O5	0.6449(3)	−0.1119(3)	0.3192(2)	0.072(1)
C1	0.8440(4)	0.2207(4)	0.0125(3)	0.074(1)
C2	0.8577(5)	0.3413(5)	0.0760(4)	0.086(1)
C3	0.6662(5)	0.4150(6)	0.0812(4)	0.102(2)
C4	0.5777(5)	0.4077(6)	0.1473(5)	0.110(2)
C5	0.4797(6)	0.2031(10)	0.1036(6)	0.155(3)
C6	0.4626(6)	0.0632(10)	0.1339(8)	0.159(3)
C7	0.5579(7)	−0.1477(8)	0.1648(4)	0.126(3)
C8	0.5568(5)	−0.1774(6)	0.2604(4)	0.103(2)
C9	0.8519(3)	−0.1333(4)	0.0852(3)	0.060(1)
C10	0.8520(4)	−0.2622(5)	0.0481(3)	0.081(1)
C11	0.8458(4)	−0.2802(6)	−0.0483(4)	0.088(1)
C12	0.8391(4)	−0.1714(5)	−0.1053(3)	0.080(1)
C13	0.8390(3)	−0.0397(5)	−0.0690(3)	0.070(1)
C14	0.8451(3)	−0.0199(4)	0.0276(2)	0.053(1)

TABLE III Atomic coordinates and equivalent isotropic displacement parameters for **2**

Atom	<i>x</i>	<i>y</i>	<i>z</i>	<i>U</i> (eq)
P1	0.7031(1)	−0.0491(1)	−0.0772(1)	0.069(1)
F1	0.6896(3)	0.0318(2)	−0.0884(2)	0.107(1)
F2	0.6351(3)	−0.0492(2)	0.0041(2)	0.112(1)
F3	0.7168(3)	−0.1302(2)	−0.0665(2)	0.111(1)
F4	0.5940(3)	−0.0609(2)	−0.1562(2)	0.104(1)
F5	0.7714(3)	−0.0507(2)	−0.1582(2)	0.118(1)
F6	0.8125(3)	−0.0388(2)	0.0012(2)	0.118(1)
N1	0.7993(3)	0.2917(2)	0.0782(3)	0.069(1)
O1	0.7077(3)	0.2834(2)	0.2659(2)	0.070(1)
O2	0.8053(3)	0.4066(2)	0.2115(3)	0.089(1)
O3	1.0106(3)	0.3572(2)	0.1669(2)	0.088(1)
O4	0.9900(3)	0.2130(2)	0.1782(3)	0.099(1)
O5	0.8959(3)	0.1733(2)	−0.0120(2)	0.082(1)
O6	0.8922(3)	0.2904(2)	−0.1032(2)	0.081(1)
O7	0.8072(3)	0.4155(2)	−0.0357(3)	0.099(1)
O8	0.5929(4)	0.3764(3)	−0.0138(4)	0.136(2)
O9	0.5878(4)	0.2322(3)	−0.0092(3)	0.113(1)
O10	0.7086(3)	0.1729(2)	0.1632(2)	0.094(1)
C1	0.7116(4)	0.3454(2)	0.3225(4)	0.077(1)
C2	0.7157(5)	0.4051(3)	0.2574(4)	0.094(2)
C3	0.9112(5)	0.4172(3)	0.2720(4)	0.096(2)
C4	0.9940(5)	0.4213(3)	0.2118(5)	0.105(2)
C5	1.0909(5)	0.3139(4)	0.2223(5)	0.114(2)
C6	1.0886(5)	0.2444(4)	0.1753(5)	0.116(2)

TABLE III (Continued)

Atom	x	y	z	U(eq)
C7	0.9774(7)	0.1418(4)	0.1502(5)	0.135(3)
C8	0.9722(7)	0.1287(4)	0.0501(5)	0.126(2)
C9	0.8995(4)	0.1696(3)	-0.1067(4)	0.077(1)
C10	0.9044(5)	0.1079(4)	-0.1528(5)	0.105(2)
C11	0.9083(6)	0.1069(5)	-0.2494(6)	0.138(3)
C12	0.9049(6)	0.1681(6)	-0.2983(5)	0.141(3)
C13	0.8999(5)	0.2303(5)	-0.2534(4)	0.114(2)
C14	0.8970(4)	0.2321(3)	-0.1546(3)	0.079(2)
C15	0.8962(5)	0.3552(3)	-0.1509(4)	0.099(2)
C16	0.9021(5)	0.4110(3)	-0.0775(5)	0.106(2)
C17	0.7155(6)	0.4453(4)	-0.0943(5)	0.119(2)
C18	0.6230(6)	0.4427(4)	-0.0452(6)	0.127(2)
C19	0.5299(9)	0.3388(5)	-0.0785(7)	0.183(5)
C20	0.4987(6)	0.2723(5)	-0.0481(6)	0.131(3)
C21	0.5612(9)	0.1731(5)	0.0275(9)	0.222(6)
C22	0.6383(8)	0.1341(4)	0.0902(5)	0.146(3)
C23	0.7017(4)	0.1633(2)	0.2567(3)	0.064(1)
C24	0.6994(4)	0.0996(3)	0.2979(5)	0.088(2)
C25	0.6944(5)	0.0929(3)	0.3933(5)	0.098(2)
C26	0.6942(5)	0.1503(3)	0.4485(4)	0.097(2)
C27	0.6985(4)	0.2157(3)	0.4091(3)	0.080(1)
C28	0.7022(3)	0.2226(2)	0.3119(3)	0.060(1)

TABLE IV Selected bond lengths [Å] and torsion angles [°] for **1**

K1-O3	2.859(3)
K1-O4	2.876(3)
K1-O2	2.877(3)
K1-O5	2.897(3)
K1-O1	2.930(3)
O1-C14	1.364(4)
O1-C1	1.436(5)
O2-C3	1.416(6)
O2-C2	1.433(6)
O3-C4	1.410(7)
O3-C5	1.406(8)
O4-C7	1.398(8)
O4-C6	1.404(9)
O5-C9#1	1.378(5)
O5-C8	1.410(5)
C1-C2	1.490(6)
C3-C4	1.508(9)
C5-C6	1.465(11)
C7-C8	1.401(8)
C14-O1-C1-C2	-173.4(3)
C3-O2-C2-C1	-77.0(5)
O1-C1-C2-O2	-63.3(5)
C2-O2-C3-C4	172.5(4)
C5-O3-C4-C3	-78.5(7)
O2-C3-C4-O3	-62.7(7)
C4-O3-C5-C6	177.2(6)
C7-O4-C6-C5	-177.3(6)
O3-C5-C6-O4	-65.8(10)
C6-O4-C7-C8	-79.4(9)
O4-C7-C8-O5	-50.3(9)
C9#1-O5-C8-C7	178.5(6)
O5#1-C9-C14-O1	1.4(5)

Symmetry code: # 1 - x + 3/2, y, - z + 1/2.

TABLE V Selected bond lengths [Å] and torsion angles [°] for **2**

O1-C28	1.356(5)
O1-C1	1.440(5)
O2-C2	1.414(6)
O2-C3	1.430(6)
O3-C5	1.411(7)
O3-C4	1.432(7)
O4-C6	1.383(7)
O4-C7	1.435(8)
O5-C9	1.359(6)
O5-C8	1.440(7)
O6-C14	1.352(6)
O6-C15	1.433(6)
O7-C17	1.389(6)
O7-C16	1.440(7)
O8-C19	1.298(9)
O8-C18	1.438(8)
O9-C20	1.372(9)
O9-C21	1.330(10)
O10-C23	1.363(5)
O10-C22	1.421(7)
C1-C2	1.490(7)
C3-C4	1.481(8)
C5-C6	1.499(9)
C7-C8	1.434(9)
C15-C16	1.494(8)
C17-C18	1.476(9)
C19-C20	1.439(12)
C21-C22	1.386(8)
C28-O1-C1-C2	-179.2(4)
C3-O2-C2-C1	-67.4(6)
O1-C1-C2-O2	-59.1(6)
C2-O2-C3-C4	-176.8(4)
C5-O3-C4-C3	-88.6(6)
O2-C3-C4-O3	-68.3(6)
C4-O3-C5-C6	171.1(5)
C7-O4-C6-C5	-170.8(5)
O3-C5-C6-O4	-66.2(7)
C6-O4-C7-C8	-68.3(8)
O4-C7-C8-O5	-48.7(9)
C9-O5-C8-C7	171.0(6)
C8-O5-C9-C14	-135.6(5)
C15-O6-C14-C9	176.4(4)
O5-C9-C14-O6	0.5(6)
C14-O6-C15-C16	-173.8(5)
C17-O7-C16-C15	-75.7(7)
O6-C15-C16-O7	-63.8(6)
C16-O7-C17-C18	176.5(6)
C19-O8-C18-C17	-82.7(9)
O7-C17-C18-O8	-55.5(9)
C18-O8-C19-C20	-179.7(8)
C21-O9-C20-C19	174.2(8)
O8-C19-C20-O9	-56.6(12)
C20-O9-C21-C22	-163.7(10)
O9-C21-C22-O10	44.3(16)
C23-O10-C22-C21	113.6(9)
C22-O10-C23-C28	-135.6(6)
C1-O1-C28-C23	-178.2(4)
O10-C23-C28-O1	1.0(6)

TABLE VI Hydrogen bonding geometry for **2** [ $\text{\AA}$  and  $^\circ$ ]

D-H...A	d(D-H)	d(H...A)	d(D...A)	<(DHA)
N1-H1N...O1	0.787(4)	2.590(3)	3.128(5)	127.1(3)
N1-H1N...O9	0.787(4)	2.385(4)	2.907(5)	124.9(3)
N1-H1N...O10	0.787(4)	2.318(4)	2.940(5)	136.6(3)
N1-H2N...O2	0.950(3)	2.199(4)	2.913(5)	131.2(2)
N1-H2N...O3	0.950(3)	2.157(3)	2.956(5)	141.0(2)
N1-H3N...O7	0.718(4)	2.242(4)	2.907(5)	154.6(3)
N1-H4N...O4	0.793(4)	2.394(4)	2.928(5)	125.6(3)
N1-H4N...O5	0.793(4)	2.260(3)	3.007(5)	157.2(3)
C22-H22A...F1	0.970(9)	2.530(3)	3.390(9)	147.8(5)
C4-H4B...F1 #1	0.970(6)	2.550(3)	3.447(7)	153.8(4)

Symmetry code: #1  $x+1/2, -y+1/2, z+1/2$ .

parameters, complete bond lengths and angles and torsion angles, and observed and calculated structure factors.

## RESULTS AND DISCUSSION

The complexes were characterized by spectral (IR and  $^1\text{H}$  NMR) and X-ray crystal structure analyses. The IR spectra of the complexes give a series of complex bands between 1260–900  $\text{cm}^{-1}$  arising from various modes of vibration of ether and methylene groups. Comparing with the spectrum of the free ligand, most of these bands are shifted to lower energy presumably due to less restriction on the coupling of some vibrational modes caused by bonding of oxygen atoms of the polyether ring with the ammonium and potassium ion, respectively. The greatest changes may be noticed in the 1000–900  $\text{cm}^{-1}$  region, which contains bands attributed to wagging, twisting and rocking modes of vibration of the methylene groups. While free DB30C10 has two strong bands at 958 and 922  $\text{cm}^{-1}$  as well as two medium bands at 938 and 909  $\text{cm}^{-1}$  associated with these vibrations, the complexes are characterized either by a medium band at 936  $\text{cm}^{-1}$  with a shoulder on the lower frequency side (complex **2**) or by two medium bands at 935 and 921  $\text{cm}^{-1}$  (complex **1**). No bands appear in the hydroxy-stretching

region over 3400  $\text{cm}^{-1}$ , indicating that complexes are not hydrated. A strong  $\nu\text{NH}_4^+$  band appears at 3256  $\text{cm}^{-1}$ .

The  $^1\text{H}$  NMR spectra of DB30C10 and its complexes show four sets of resonant signals for the methylene and two sets for the aromatic protons (see Fig. 1). Two separated multiplets in the aromatic region are due to the AA'BB' coupling network typical for the 1, 2-disubstituted benzenes. A similar coupling pattern is found also for protons of the 3- $\text{CH}_2$  and 4- $\text{CH}_2$  groups. Comparing with the spectrum of the free ligand there are no great chemical shift differences in complexes, which could be ascribed to great solvating ability of DMSO and its interaction not only with the cation, but also with the ligand molecule. In the potassium complex the 4- $\text{CH}_2$  and aromatic protons are shifted downfield by 3.5 Hz, 1- $\text{CH}_2$  by 2 Hz, while 3- $\text{CH}_2$  and 2- $\text{CH}_2$  protons show an upfield shift of 2 Hz. Similarly, in the ammonium complex the 4- $\text{CH}_2$  protons are shifted slightly downfield by 3 Hz, 3- $\text{CH}_2$  protons are shifted upfield to the same extent, while resonances of the 1- $\text{CH}_2$  and 2- $\text{CH}_2$  protons as well as the aromatic protons are essentially unchanged upon complex formation. The NOESY spectrum of this complex indicates a relatively strong cross-peak between the ammonium protons and DMSO. Besides interactions between the neighbour protons within the aromatic as well as the

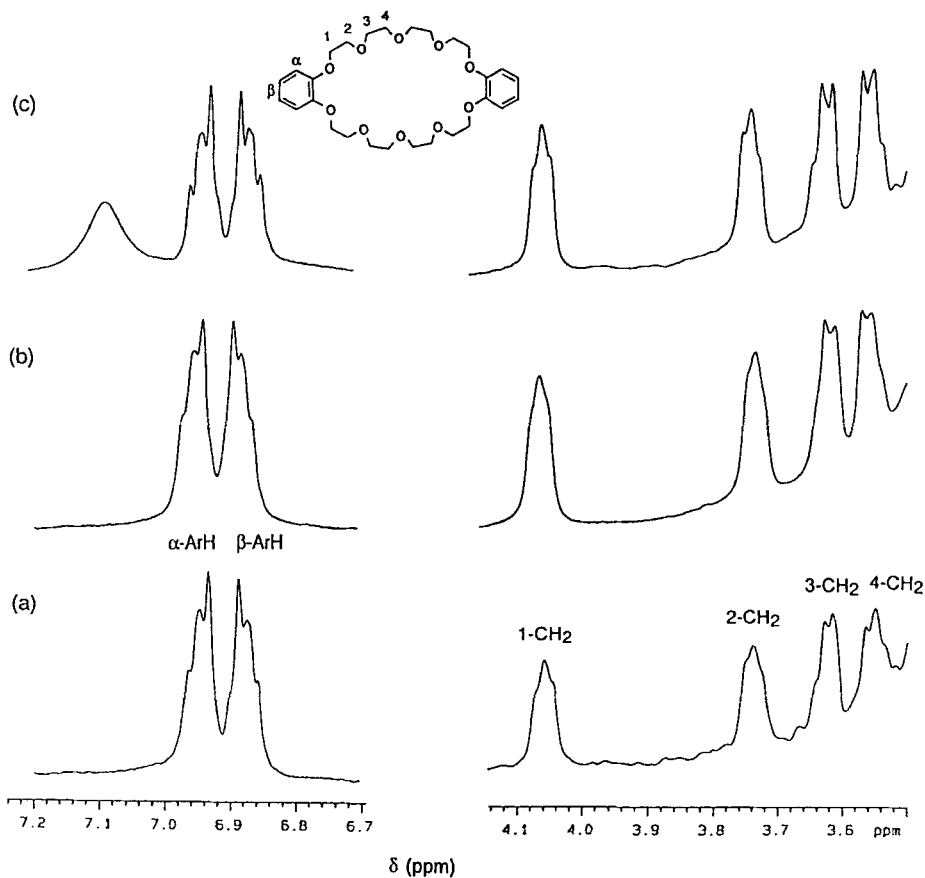


FIGURE 1  $^1\text{H}$  NMR spectra in  $\text{DMSO-d}_6$  showing the ether methylenic and aromatic regions: (a) DB30C10, (b)  $\text{K}(\text{DB30C10})\text{PF}_6$ , and (c)  $\text{NH}_4(\text{DB30C10})\text{PF}_6$ .

methylene protons, the main inter-ligand NOESY cross-peak is that between the  $\alpha$ -ArH and 1- $\text{CH}_2$  protons.

The X-ray structure analyses show that the asymmetric unit of compound **1** consists of  $[\text{K}(\text{DB30C10})]^+$  cation and hexafluorophosphate anion. The ORTEP view with the numbering scheme of cation is given in Figure 2, while packing in the unit cell is presented in Figure 3. The potassium atom (as well as P1, F1 and F2 atoms) is situated on a twofold axis and is completely encapsulated with the polyether ring coordinated to the ten oxygen atoms. The K–O distances range from 2.859(3) to 2.930(3) Å, which corresponds to the sum of the ionic radius

of  $\text{K}^+$  for coordination number 10 (1.59 Å) [23] and the van der Waals radius of O atom (1.40 Å). A similar value was found in DB30C10·KI complex with 2.850(6)–2.931(6) Å [4]; or 2.857(2)–2.935(2) Å in DB30C10·KSCN complex [6], and 2.861(6)–3.106(7) Å in DB30C10·KSCN· $\text{H}_2\text{O}$  complex [6].

In compound **2** the crown ether ring completely encapsulates the ammonium cation (Fig. 4). Using the criterion that a hydrogen bond exists when the  $\text{H}\cdots\text{O}$  distance is less than 2.4 Å [24] (0.2 Å less than the sum of the van der Waals radii of H and O), it can be seen that four H atoms of the ammonium cation are involved in seven hydrogen bonds (Tab. VI). In addition, the



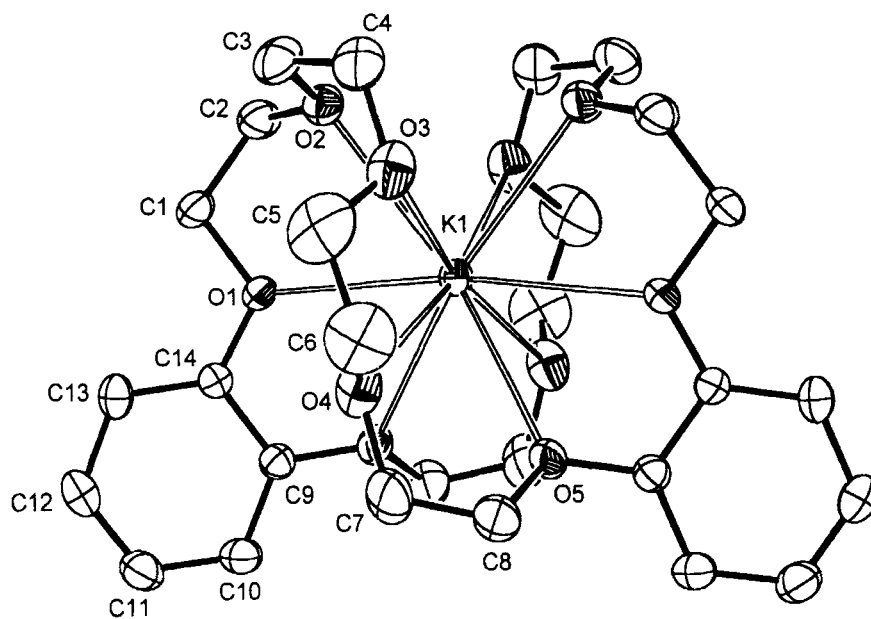
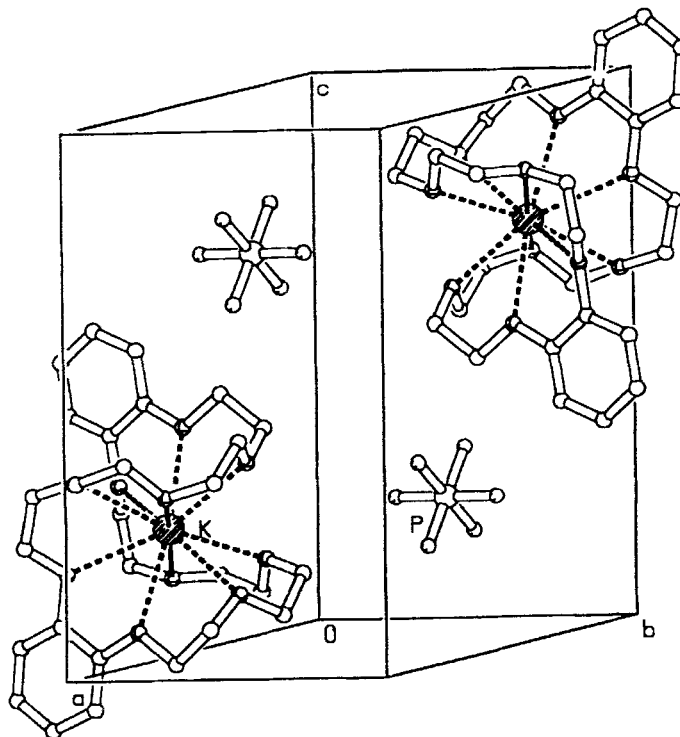
FIGURE 2 ORTEP view of [K(DB30C10)]<sup>+</sup> cation with atom numbering in complex 1.

FIGURE 3 Packing in the unit cell for 1.

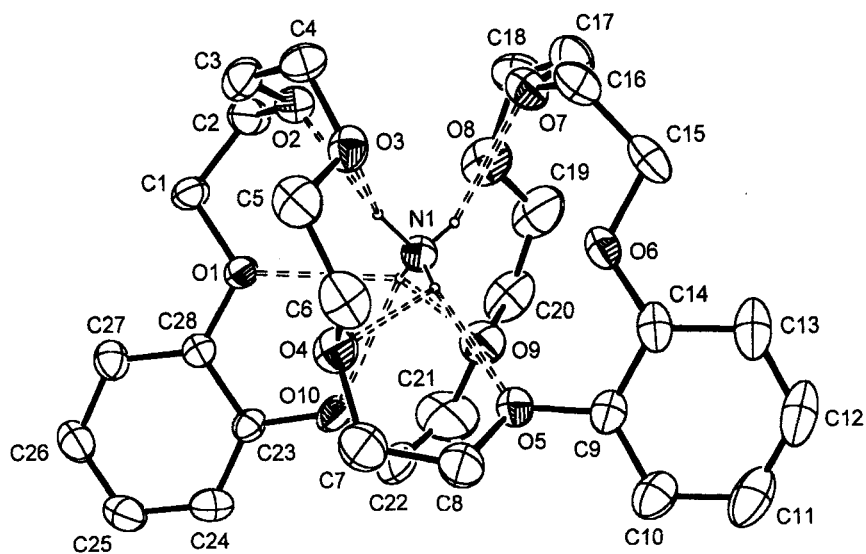
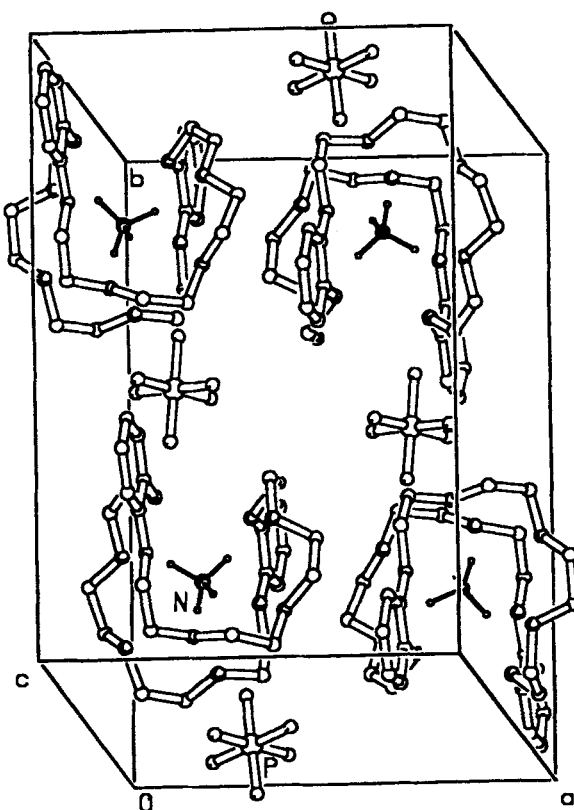
FIGURE 4 ORTEP view of  $[\text{NH}_4(\text{DB30C10})]^+$  cation with atom numbering in complex 2.

FIGURE 5 Packing in the unit cell for 2.

H1N atom also interacts very weakly with O1 at the distance:  $N1 \cdots O1 = 3.128(5) \text{ \AA}$ ;  $H1N \cdots O1 = 2.590(3) \text{ \AA}$  and the angle  $N1-H1N \cdots O1$  of  $127.1(3)^\circ$ .

Bond distances  $C(sp^3)-C(sp^3)$ , ranging from  $1.401(8)$  to  $1.508(9) \text{ \AA}$  in complex **1** (Tab. IV) and from  $1.386(8)$  to  $1.499(9) \text{ \AA}$  in complex **2** (Tab. V), are too short for the expected single C–C bond. Distances  $C(sp^3)-O$  are from  $1.398(8)$  to  $1.436(5) \text{ \AA}$  in compound **1** and from  $1.298(9)$  to  $1.440(7) \text{ \AA}$  in compound **2**. This systematic effect for both types of bonds in the crown ether ring was found in all the crystal structures of cyclic and open polyethers and in their complexes with cations as well as with neutral guests. Formerly, this feature was believed to be caused by inadequate treatment of thermal vibrations during the refinement procedure [25]. However, the structural analysis at a temperature of 100 K found only slightly increasing of  $0.005 \text{ \AA}$  with respect to the room temperature structure [26].

In many crystal structures a high degree of thermal motions for some atoms in the different crown ring is also observed. We found this in complex **1** for C5 and C6 atoms and in complex **2** for C19, C21 and C22 atoms. In ammonium complex the influence on the values of related bond distances was very remarkable. Any attempt to make some improvement in refinement (finding positions of atoms on  $\Delta F$  maps or suggested splitting by program) was without success. We then refined the C21–C22 distance with a constraint length at the value of  $1.386(8) \text{ \AA}$ . The O8–C19 length is unusually short –  $1.298(9) \text{ \AA}$ . Maybe that could be a consequence of making maximum possible hydrogen bonds with  $NH_4^+$  cation. A very similar pattern of disorder and identical short bond lengths were reported in potassium and rubidium thiocyanate complexes with DB30C10 [5–7].

There are two short C–H $\cdots$ F contacts in compound **2** that occur with aliphatic carbon atoms:  $C4-H4B \cdots F1 [x+1/2, -y+1/2, z+1/2] = 3.447(7) \text{ \AA}$  with  $H4B \cdots F1 = 2.550(3) \text{ \AA}$  and an angle of  $153.8(4)^\circ$  and  $C22-H22A \cdots F1$

$3.390(9) \text{ \AA}$  with  $H22A \cdots F1 = 2.530(3) \text{ \AA}$  and an angle of  $147.8(5)^\circ$ . The last contact involves exactly the C22 atom, which exhibits great thermal motion and a very short distance to the C21 atom.

The most interesting feature of these structures is the conformation of the polyether ring. Sequential units O–CH<sub>2</sub>–CH<sub>2</sub>–O have minimum energy with torsion angles about C–C bonds being *gauche* or *synclinal* ( $60^\circ$ ) and about C–O bonds being *anti* or *antiperiplanar* ( $180^\circ$ ). These preferences make an *anti, gauche, anti (a, g, a)* sequence for endocyclic torsion angles, with a possibility of *gauche* angles being  $g^+$  or  $g^-$ . However, it does not preclude deviations if required by ring formation or cation complexation. The latter process may cause major distortions of C–O torsion angles whereas C–C bonds are essentially *synclinal* (“all-*gauche* conformation”).

Since this convention does not illustrate numerical differences very precisely and tables with torsion angles are not very popular, we prefer to use a polar coordinate map for comparison of different crown conformations. According to the original paper [27] we make some changes in the presentation of these angles which are very useful for crown ethers. It diminishes the small differences about *anti* torsion angles ( $+175$  vs.  $-175^\circ$ ) and accentuates the equal small differences between *synperiplanar* torsion angles ( $+5$  vs.  $-5^\circ$ ). The former is very common in crown ethers, while the latter occurs very rarely. We found this procedure particularly effective when applied to large ring systems because it permits immediate recognition of similarities and differences between related conformations. The other use of polar coordinate maps is perception of symmetry elements.

The torsion angles in **1** and **2** are listed in Tables IV and V and the conformations of polyether rings are shown by polar coordinate maps in Figure 6. The starting point of these maps was chosen at the C–O1–C1–C2 torsion

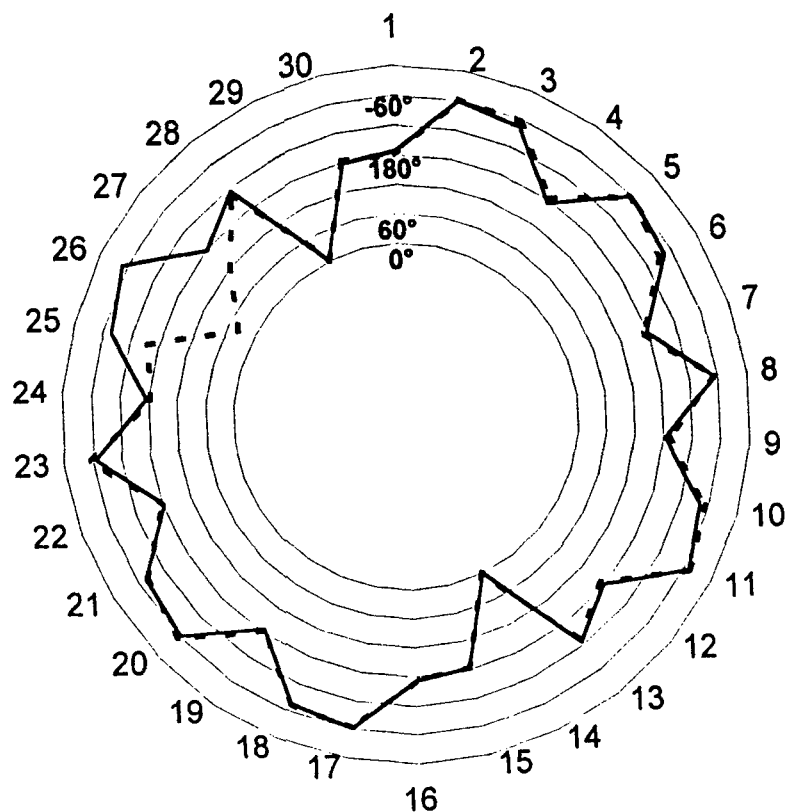


FIGURE 6 Polar coordinate maps of the macrocyclic rings in 1 (heavy line) and 2 (dashed line).

angle. It is obvious that the differences occur at angles 25, 26 and 27 in the O9–C21–C22–O10 part of the macrocyclic ring. These torsion angles have the following value:  $-79$ ,  $-50$ ,  $178^\circ$  in **1** and  $-164$ ,  $44$ ,  $114^\circ$  in **2**. The conformation of dibenzo-30-crown-10 in potassium complex (**1**) exhibits a crystallographic  $C_2$  symmetry.

Comparison with previously reported dibenzo-30-crown-10 complexes shows the identical conformation of the polyether ring in complex with potassium iodide [4] and with potassium thiocyanate [6]. It is shown in an overlay of the polar maps in Figure 7, which also exhibits crystallographic twofold axes. Figure 8 gives a polar coordinate map of crown conformation in potassium thiocyanate monohydrate complex [6], which is isomorphous with rubidium thiocyanate monohydrate complex. The principal

differences occur in torsion angles denoted here as 2 and 3. Angle 2 is an O–C–C–O torsion angle, which has switched sign from *gauche*<sup>-</sup> to *gauche*<sup>+</sup>. This is accompanied by a change in the C–C–O–C torsion angle at bond 3 from *gauche*<sup>-</sup> to *anti*. A much smaller change is evident at angle 30; from *anti* in monohydrated thiocyanate complex to  $-120^\circ$  in the anhydrous form of thiocyanate complex.

We can now compare the conformations of the crown ring in this work (Fig. 6) with the conformations in Figure 7. The main differences are in torsion angles 6, 7, 21 and 22 with the changes from *gauche*<sup>-</sup>, *anti*, *gauche*<sup>-</sup>, *anti* for our structures to *anti*, *gauche*<sup>-</sup>, *anti*, *gauche*<sup>-</sup> in KI and KSCN complexes. The minor changes are at torsion angles 13, 15, 28 and 30 from  $-130^\circ$ , *anti*,  $130^\circ$ , *anti* in the former to *anti*,  $120^\circ$ , *anti*,  $-130^\circ$  in the latter ones.

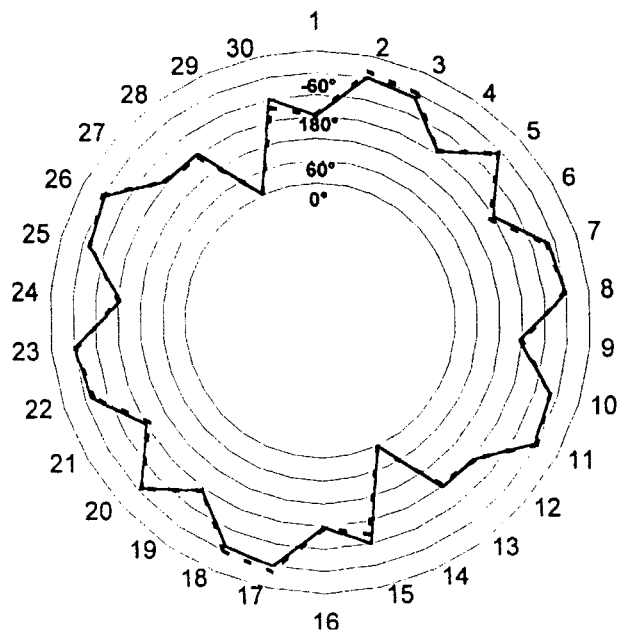


FIGURE 7 Polar coordinate maps of the macrocyclic rings in DB30C10·KSCN complex (heavy line) and DB30C10·KI complex (dashed line).

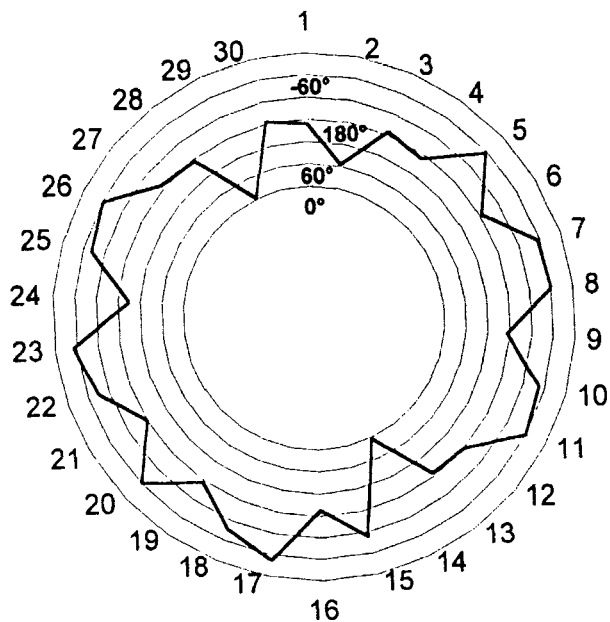


FIGURE 8 Polar coordinate map of the macrocyclic ring in DB30C10·KSCN·H<sub>2</sub>O complex.

For comparison we also present the ellipsoidal conformation of uncomplexed dibenzo-30-crown-10 molecule [4] in a polar map (Fig. 9).

Here we switch the sign of the reported value for O–C (arom.)–C(arom.)–O torsion angle, denoted as 14, from *synperiplanar*<sup>-</sup>

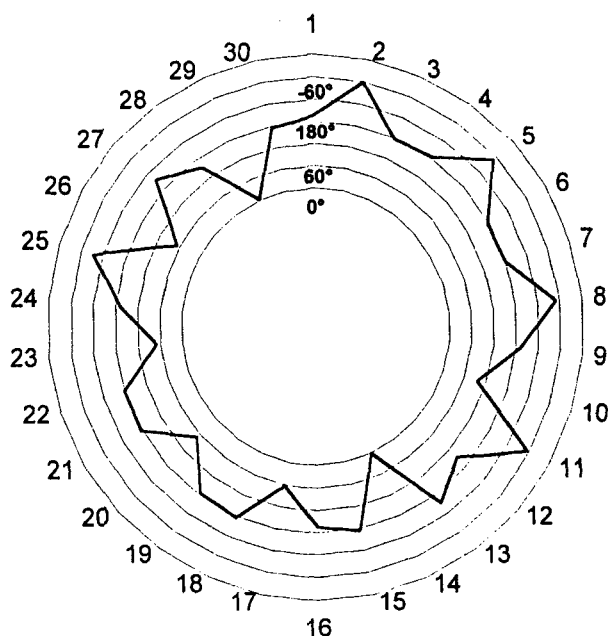


FIGURE 9 Polar coordinate map for uncomplexed dibenzo-30-crown-10 ether.

to *synperiplanar*<sup>+</sup> to avoid possible confusion.

## CONCLUSION

In potassium and ammonium hexafluorophosphate complexes with dibenzo-30-crown-10, the ligand ring completely wraps around the cation leading to very effective three-dimensional encapsulation. Both cations are of the same size: radius  $\text{NH}_4^+$  is 1.48 Å [28], while the radius of  $\text{K}^+$  (for coordination 10) is 1.59 Å. The resulting conformations of the DB30C10 ring differ only in three torsion angles. This type of conformation is often called a "tennis ball seam" or "nesting" conformation. The comparison of the conformation of the large and flexible DB30C10 ring with related conformation of the crown in ours and previously reported potassium complexes exhibits a similar pattern of molecular recognition to that achieved in naturally occurring antibiotics valinomycin [29,30]

or nonactin [31] and their complexes with  $\text{K}^+$  [32,33].

## Acknowledgements

The financial support granted by the Ministry of Science, Technology and Informatics of the Republic of Croatia is gratefully acknowledged. Lj. T-B thanks Mr. Ž. Marinić and Mrs. B. Metelko (Institute Ruder Bošković) for recording the NMR spectra. Crystal data available from the authors on request.

## References

- [1] Lamb, J. D., Izatt, R. M. and Christensen, J. J. (1981). *Stability Constants of Cation-Macrocyclic Complexes and Their Effect on Facilitated-Transport Rates*, Chapter 2 In: *Progress in Macrocyclic Chemistry*, 2, Izatt, R. M. and Christensen, J. J. (Eds.), Wiley-Interscience, New York.
- [2] Blake, A. J. and Schroeder, M. (1993). *Adv. Inorg. Chem.*, 35, 2.
- [3] Gokel, G. W. (1991). *Crown Ethers and Cryptands*, The Royal Society of Chemistry, Cambridge, England.

- [4] Bush, M. A. and Truter, M. R. (1972). *J. Chem. Soc., Perkin. Trans.*, **2**, 345.
- [5] Hašek, J., Hlavata, D. and Huml, K. (1980). *Acta Cryst.*, **B36**, 1782.
- [6] Owen, J. D., Truter, M. R. and Wingfield, J. N. (1984). *Acta Cryst.*, **C40**, 1515.
- [7] Hašek, J., Hlavata, D. and Huml, K. (1979). *Acta Cryst.*, **B35**, 330.
- [8] Li, Zen-Qian, Xu, Hong-Wei, Wang, Xiu-Weng and Fan, Yue-Peng (1989). *Jiegou Huaxue (J. Struct. Chem.)*, **8**, 273.
- [9] Fan, Yue-Peng, Xu, Hong-Wei, Wei, Yun-He and Hu, Qing-Ping (1991). *Shandong Dax. Xuebao, Zir. Kex. (J. Shandong Univ.)*, **26**, 129.
- [10] Amini, M. K. and Shamsipur, M. (1991). *Inorg. Chim. Acta*, **183**, 65.
- [11] Owen, J. D. and Truter, M. R. (1979). *J. Chem. Soc., Dalton Trans.*, p. 1831.
- [12] Junk, P. C. and Atwood, J. L. (1997). *J. Chem. Soc., Dalton Trans.*, p. 4393.
- [13] Tušek-Božić, Lj. (1987). *Electrochim. Acta*, **32**, 1579.
- [14] Dapporto, P., Paoli, P., Matijašić, I. and Tušek-Božić, Lj. (1996). *Inorg. Chim. Acta*, **252**, 383.
- [15] Dapporto, P., Paoli, P., Matijašić, I. and Tušek-Božić, Lj. (1998). *Inorg. Chim. Acta*, **282**, 76.
- [16] Kay, R. L., Zawoyski, C. and Evans, D. F. (1965). *J. Phys. Chem.*, **69**, 4208.
- [17] Yeager, H. L. and Kratochvil, B. (1975). *Can. J. Chem.*, **53**, 3448.
- [18] Altomare, A., Cascarano, G., Giacovazzo, C., Guagliardi, A., Burla, M. C., Polidori, G. and Camalli, M. (1994). *J. Appl. Crystallogr.*, **27**, 435.
- [19] Sheldrick, G. M. (1997). *SHELXL97, Program for the refinement of crystal structures*, University of Goettingen, Germany.
- [20] Walker, N. and Stuart, D. (1983). *Acta Cryst.*, **B39**, 158.
- [21] Farrugia, L. J. (1998). *ORTEP-3 for Windows*, Version 1.03, University of Glasgow, Glasgow, Scotland, UK.
- [22] Speck, A. L. (1998). *PLATON-98*, University of Utrecht, Utrecht, The Netherlands.
- [23] Schannon, R. D. (1976). *Acta Cryst.*, **A32**, 751.
- [24] Jeffrey, G. A. (1995). *Cryst. Rev.*, **4**, 211.
- [25] Dunitz, J. D. and Seiler, P. (1974). *Acta Cryst.*, **B30**, 2739.
- [26] Maverick, E., Seiler, P., Schweizer, W. B. and Dunitz, J. D. (1980). *Acta Cryst.*, **B36**, 615.
- [27] Ounsworth, J. P. and Weiler, L. (1987). *J. Chem. Education*, **64**, 568.
- [28] Suzuki, E., Muta, T., Nozaki, R. and Shiozaki, Y. (1996). *Acta Cryst.*, **B52**, 296.
- [29] Karle, I. L. (1975). *J. Am. Chem. Soc.*, **97**, 4379.
- [30] Smith, G. D., Duax, W. L., Langs, D. A., DeTitta, G. T., Edmonds, J. W., Rohrer, D. C. and Weeks, C. M. (1975). *J. Am. Chem. Soc.*, **97**, 7242.
- [31] Dobler, M. (1972). *Helv. Chim. Acta*, **55**, 1371.
- [32] Neupert-Laves, K. and Dobler, M. (1975). *Helv. Chim. Acta*, **58**, 432.
- [33] Kilbourn, B. T., Dunitz, J. D., Pioda, L. A. R. and Simon, W. (1967). *J. Mol. Biol.*, **30**, 559.